AIP | Journal of Renewable and Sustainable Energy

Physicochemical properties and hygroscopicity of tobacco stem biochar pyrolyzed at different temperatures

Hanping Chen, Guiying Lin, Xianhua Wang, Yingquan Chen, Yingpeng Liu, Haiping Yang, and Jingai Shao

Citation: Journal of Renewable and Sustainable Energy **8**, 013112 (2016); doi: 10.1063/1.4942784
View online: http://dx.doi.org/10.1063/1.4942784
View Table of Contents: http://scitation.aip.org/content/aip/journal/jrse/8/1?ver=pdfcov
Published by the AIP Publishing

Physicochemical properties and hygroscopicity of tobacco stem biochar pyrolyzed at different temperatures

Hanping Chen, Guiying Lin, Xianhua Wang,[a] Yingquan Chen, Yingpeng Liu, Haiping Yang, and Jingai Shao
State Key Laboratory of Coal Combustion, Huazhong University of Science and Technology, Wuhan 430074, China

(Received 13 July 2015; accepted 12 February 2016; published online 25 February 2016)

The physicochemical properties and hygroscopicity of biochar derived from tobacco stem pyrolysis were investigated to get the effect of pyrolysis temperature (250–950 °C). The chemical composition and structure of biochar were characterized with proximate and ultimate analysis, X-ray fluorescence, and two-dimensional perturbation-based correlation infrared spectroscopy (2D-PCIS) based on Fourier-transform infrared spectroscopy. The physical pore structure was analyzed by Brunauer-Emmett-Teller surface area. Results showed that surface area and pore volumes of biochar increased, while biochar yield, volatile matter, H/C and O/C ratios decreased with the increasing pyrolysis temperature. The 2D-PCIS analysis suggested that the intensity of hydroxyl groups and aromatic skeletal changed greatly with pyrolysis temperature. Tobacco stem biochar was abundant in Ca and K and contained P, Mg, S, and Cl, while N was low and decreased with temperature. Tobacco stem biochar produced at 550 °C has the lowest hygroscopicity under 50%–70% humidity. Biochar produced from tobacco stem may not be suitable to be used as fuel while it can be developed for soil amendment and adsorbent by optimizing pyrolysis conditions and modifications.
 [http://dx.doi.org/10.1063/1.4942784]

I. INTRODUCTION

Biochar is the solid product from thermochemical conversion of biomass in a limited or no oxygen atmosphere.[1] Biochar can be used as a soil amendment to improve soil conditions and retain soil water and nutrients,[2] thus improving the production and quality of crops.[3,4] Simultaneously, it shows the advantage of carbon sequestration and greenhouse gases reduction. It was reported that biochar contained stable carbon, and it can lead to carbon sequestration of about 50% of the initial carbon compared to combustion and biological decomposition of biomass.[5,6] Additionally, biochar also shows high porosity, and can be used as adsorbent for pollutants, such as heavy metal and pesticides.[7,8]

The potential application of biochar is mainly dependent on the physicochemical properties, which are mainly affected by the production conditions of biochar and its feedstock characteristics.[9–11] Pyrolysis conditions such as temperature, heating rate, reaction time, and pyrolysis atmosphere play critical roles in the yield and quality of biochar.[12,13] Temperature is the major factor, which has gained wide consideration. Zheng *et al.*[14] investigated the impact of pyrolysis temperature (300–600 °C) on basic properties and nutrient transformation of giant reed biochar, and found that low-temperature biochars (≤400 °C) showed higher nutrient availability. Al-Wabel *et al.*[15] found that biochar obtained at high temperature may have a higher carbon sequestration potential while biochars produced at low temperature have preferred an impact on soil with high alkalinity, high salinity, and low organic matter content in the arid regions. However, the optimization of biochar production under various

[a]Electronic mail: wxhwhhy@sina.com. Tel.: 86-27-87559358. Fax: 86-27-87545526.

temperatures was not enough to provide the features of biochar for its application. Novak *et al.*[16] pointed out that biochar may be regulated to selectively improve the physicochemical properties of soil by altering pyrolysis conditions and feedstocks. Therefore, the study of physicochemical properties in biochar obtained from different pyrolysis temperatures for some biomass would be significant on the effective use of biomass and improving the application value of biochar.

Tobacco stem is the typical byproduct during the manufacturing process of tobacco, which will be harmful to the environment and human health without appropriate and valid utilization. Pyrolysis of tobacco stem, an effective utilization option, offers different products such as biogas, bio-oil, and biochar with higher application value. Tobacco waste has higher ash and lower fixed carbon than pine cone, soybean cake, corn stalk, and peanut shells,[17,18] which may result in the potential and special application of tobacco. Much of the study on pyrolysis of tobacco is focused on the behavior and kinetics of pyrolysis,[19] as well as the analysis of biogas and bio-oil.[20,21] Strezov *et al.*[22] studied the pyrolysis behavior of tobacco leaves in the form of dust and revealed the four stage pyrolysis mechanism (dehydration-200 °C, torrefaction-300 °C, charring-500 °C, and carbonization-750 °C). It was also found that biogas had reasonably high calorific value for generating energy, bio-oil with complex chemical structure, and biochar contained large concentration of potassium.

There is little literature on physicochemical properties of tobacco stem biochar. Particularly, the hygroscopicity of tobacco stem biochar has been rarely discussed; however, it is critical to biochar applications such as retaining water and nutrients of soil and adsorbing pollutants. Karhu *et al.*[23] mentioned that the water holding capacity was increased by 11% with birch biochar addition. The hygroscopicity and water retention capacity of biochar maybe attributed to its porous structure, functional group, and other factors.[24,25] Hence, it will be of great importance to study the physicochemical properties and hygroscopicity of biochar for its agriculture and environment applications.

In this work, the characteristics of tobacco stem biochar produced at different temperatures were investigated using the proximate and ultimate analysis, Fourier transform infrared (FTIR) spectroscopy, Brunauer-Emmett-Teller (BET) surface area, and with X-ray fluorescence (XRF). The hygroscopicity experiment of tobacco stem biochar was done by the gravimetric method at different relative humidity from 50% to 90% and constant temperature 30 °C. The aims of this study were to evaluate the effects of pyrolysis temperature on the physicochemical properties and hygroscopicity of tobacco stem biochar.

II. EXPERIMENTAL

A. Sample

Tobacco stem obtained from local regions was used as raw materials. The tobacco stem was air dried and ground to sieve through a 60 mesh screen. The proximate analysis of tobacco stem showed that it contained volatile matter 67.18%, higher ash 16.93%, and lower fixed carbon 4.76% on air dried basis. The carbon, hydrogen, and nitrogen contents were 32.47%, 4.5%, and 2.44%, respectively, and the oxygen content is 32.44% by difference. Tobacco stem had higher chlorine, calcium, and potassium, along with trace elements of copper, iron, manganese, and titanium oxides. Tobacco stem growth absorbed various nutrients from soil as inherent nutrient elements in tobacco stem which can be recycled for agricultural applications (Table I).

TABLE I. The contents of element oxides in tobacco stem by XRF (%).

	Cl_2O	CaO	K_2O	SO_3	MgO	P_2O_5	CdO	Al_2O_3
TS	10.52	8.57	7.12	6.14	3.34	2.47	1.27	1.26

B. Biochar production

Biochar was produced from tobacco stem pyrolysis in a tubular reactor at temperatures variant from 250 °C to 950 °C with nitrogen (600 ml/min) for 40 min. The reactor consisted of a quartz tube (internal diameter 38 mm, length 600 mm) and thermocouple placed in the middle of the reactor to measure the reaction temperature. When the tubular reactor was heated up to the desired temperature with the heating rate of 10 °C/min, about 6 g samples in three porcelain crucibles were pushed rapidly into the center of the tube. Biochar was moved to low temperature section of the tube for compulsory cooling by a fan when the pyrolysis reaction was completed and cooled down with nitrogen to ambient temperature. The biochar yield was calculated from the product amount in porcelain crucible based on the mass of feedstock. Each experiment was carried out with duplicates, and the final yield of biochar provided was the average value with experimental error less than ±1.0%. Biochars produced at different temperatures were labeled as TS250, TS350,…, TS950.

C. Biochar properties

Proximate analysis of tobacco stem biochar was conducted in an industrial analyzer (Vario EL-2, Germany). Elemental C, N, and H were determined directly using an elementary analyzer (Vario Micro cube, Germany) via high-temperature combustion method, and oxygen content was obtained by difference. Low heating value (LHV) of each sample was measured by an automatic calorimeter instrument (Parr 6300, USA).

Tobacco stem biochar was measured with the FTIR spectra (a VERTEX 70 spectrometer, Bruker, Germany) to study the effect of temperature on surface organic functional groups. Samples were first mixed with KBr (1:200, w/w) and ground, and then pressed into pellets. Each sample was scanned from 400 to 4000 cm^{-1} wave numbers at a resolution of 2 cm^{-1}. Two-dimensional Correlation Spectroscopy[26,27] was used to determine main functional groups in biochar according to FTIR of biochar.

XRF measurements were used to obtain chemical element compositions of tobacco stem biochar. The XRF spectrometer (EAGLE III, America EDAX, Inc.) can provide the content and distribution of the sample with the atomic number of element higher than sodium. The samples were pre-dried and pasted onto a white optical disk to eliminate potential interferences of context.

The BET surface area (S_{BET}), micropore volume (V_{mic}), and total pore volume (V_{total}) of biochar were obtained by an automatic adsorption analyzer (ASAP 3000, USA). To obtain the pore structure, biochar samples were first degassed under vacuum for 24 h at 150 °C, and the adsorption-desorption isotherms were measured by liquid nitrogen adsorption at 77 K.[28]

D. Moisture sorption measurements

The hygroscopicity property of biochar was conducted in a constant temperature and humidity incubator (HWS-150, China) based on the gravimetric method. The moisture sorption characteristics were analyzed at different relative humidity conditions from 50% to 70% and constant temperature 30 °C. About 1 g of biochar particles was placed evenly at the bottom of the weighing bottle with a diameter of 50 mm and height 35 mm. First, the weighed samples were dried in an oven at 105 °C for 12 h and the weight was recorded after samples cooling to room temperature in a desiccator. Then sample bottles were placed in the incubator which had met the set test conditions, and bottle without the sample was set as a control to check the impact of incubator humidity on the weighing bottle. For all experiments, the change in the weight of the bottles contained samples with time by digital balance 200 ± 0.0001 g. Experiment was considered to reach equilibrium when the change in the weight did not exceed 0.001 g for three successive weighing.

Moisture content (MC) of a sample at each relative humidity was calculated according to the measured weight. Each experimental treatment was done with triplicates and average values were taken. The average of the last three moisture contents in equilibrium is regarded as

equilibrium moisture content (EMC) of samples. After the experiment, the samples were dried in an oven (105 °C for 12 h) to obtain dry matter.

III. RESULTS AND DISCUSSION

A. Yield and composition of biochar

The effects of pyrolysis temperature on biochar yield and composition are given in Table II. The yield of tobacco stem biochar decreased rapidly from 52.39% to 30.98% with temperature increasing from 250 °C to 650 °C as the degradation of tobacco stem mainly took place among 250–650 °C. Then biochar yield decreased slowly till temperature higher up to 950 °C as the secondary cracking of organic residue in solid biochar samples. LHV indicates the potential use for the energy available. The LHV of tobacco stem biochar decreased from the maximum value (14.30 MJ/kg) at 250 °C to the minimum value (9.64 MJ/kg) at 650 °C and then increased with pyrolysis temperature. It was found that LHV of tobacco stem was similar to that of cotton stalk (11.629 MJ/kg).[29] However, LHVs of cotton stalk biochars with minimum value of 20.53 MJ/kg were much higher than that of the tobacco stem biochars. The reason may be that tobacco stem biochars have higher volatile matter and ash. Tobacco stem biochars with lower LHV are inadvisable to be used as fuel.

The volatile matter content of biochar decreased from 53.65% to 34.02% when pyrolysis temperature increased. The results showed that volatile matter of tobacco stem is removed by pyrolysis process. The ash content of biochar first increased and then decreased with increasing pyrolysis temperature, and the maximum content was 44.71% at 650 °C. The ash content in biochar was much higher than that of feedstock, mainly because ash transformed from the mineral matter accumulated in biochar.[30] It is regarded that the high silica content of biomass may explain the high ash content of biochar which is a measure of the non-combustible component and non-volatile matter in biochar.[15,28] Above 750 °C, the matters resistant to disintegration were further decomposed resulting in the decrease of the ash. The volatile matter and ash content of tobacco stem biochar were higher than those of biochar produced from corn stalk and peanut shell[18] at the same temperature, while tobacco stem biochar contained lower fixed carbon content.

Nitrogen was the major nutrient element for plants, and tobacco stem had higher nitrogen content than corn stalk and peanut shell.[18] The changes of nitrogen content in tobacco stem biochar produced at pyrolysis temperature below 550 °C were not obvious, due to the low volatilization of N-contained compounds during pyrolysis. The nitrogen content in high temperature biochars significantly decreased, and it indicated that the N-contained functional groups mainly

TABLE II. Effect of pyrolysis temperature on yield and composition of biochar.

		Pyrolysis temperature (°C)					
Parameters	TS	250	350	450	550	650	750
Yield (%)	…	52.39	43.57	38.47	35.46	30.98	29.98
LHV(MJ/kg)	11.80	14.30	13.33	12.05	11.31	9.64	9.79
Proximate analysis (wt. %, d)							
VM	67.18	53.65	46.96	42.71	41.59	41.75	34.04
Ash	16.93	28.15	32.85	38.68	42.31	44.71	42.79
FC	4.76	8.92	10.76	9.74	8.74	4.14	13.65
Ultimate analysis (wt. %, d)							
C	32.47	38.32	37.1	35.95	35.99	32.39	32.85
H	4.59	3.57	3.09	2.14	1.48	1.27	1.18
N	2.44	2.90	2.54	2.33	2.06	1.92	1.80
O	32.44	17.79	14.99	12.03	10.81	10.3	11.85

disintegrated under high temperature. The carbon content in biochar was higher than that in tobacco stem while the hydrogen and oxygen contents were the opposite. The relationship between H/C and O/C in the form of van Krevelan diagram is given in Fig. 1. H/C and O/C of tobacco stem are much higher than its biochar produced at 250–950 °C due to the low aromaticity in tobacco stem. The high H/C and O/C ratios of raw tobacco stem and its biochar at lower pyrolysis temperatures show that it is polar and more interactive with water.[16] The H/C and O/C of biochar decreased rapidly and became relatively constant at higher temperature, and it indicated that the aromatic structure of the tobacco stem biochar increased with the increase of temperature and highly developed at temperature more than 550 °C. The pyrolysis temperature had a significant impact on the yield and composition of biochar.

B. Characteristics of biochar

1. Pore structure of biochar

The adsorption and desorption isotherms of nitrogen at 77 K for tobacco stem biochar are given in Fig. 2. TS950 has the highest nitrogen adsorption quantity, followed by TS850, TS750, and TS650, while the sorption capacity of biochar produced at pyrolysis temperature lower than 550 °C is relatively low. The sorption capacity of tobacco stem biochar produced at higher temperature increases markedly with relative pressure. The isotherm shapes of biochars are different with the transition between 550 °C and 650 °C. The isotherms of tobacco stem biochar derived at temperature higher than 650 °C are the type II while lower than 650 °C are type III, according to IUPAC classifications.[31] The biochar isotherms are of type II indicating that the biochar samples are mainly micropores which contribute much to the specific surface area. The type III isotherm shows that the adsorbate-adsorbate interactions play an important role on nitrogen sorption. The hysteresis between the adsorption and desorption isotherms in tobacco stem biochar becomes more apparent with the increased pyrolysis temperature. Hysteresis is generally associated with capillary condensation in mesopore structures, and it can be concluded that higher temperature biochar had more mesopores than lower temperature biochar.

The BET surface area (S_{BET}), average pore width, and pore volumes including micropore (V_{micro}) and total pore (V_{total}) of tobacco stem biochars are presented in Table III. The surface area of tobacco stem biochar increased with pyrolysis temperature and it increased quickly as temperature increased from 750 °C to 850 °C. The variation trend of biochar surface area was

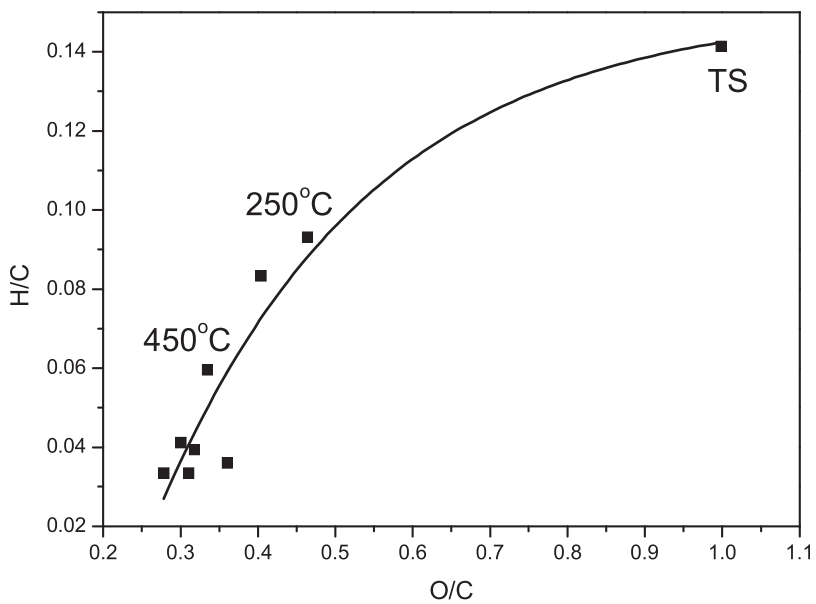

FIG. 1. van Krevelan diagram for tobacco stem biochar.

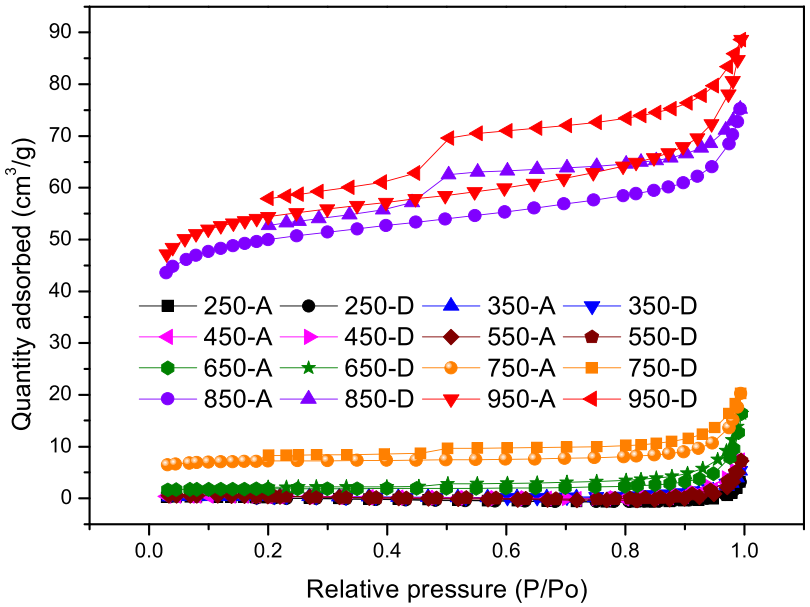

FIG. 2. N_2 adsorption and desorption isotherms at 77 K for tobacco stem biochar.

different from that reported by Sharma,[32] who found that the surface area increased to a maximum of 8 m^2/g at 400 °C and then decreases. The differences in biochar surface area might be due to the pyrolysis conditions and characteristics of tobacco. The carrier gas used by Sharma was helium for pyrolysis while it was nitrogen in this study. In addition, the sample, a mixture of tobaccos, had lower ash content (12.9%) and higher carbon content (50.6%).

The surface areas of biochars below 550 °C were quite low (0.2–1.18 m^2/g) with the minimum value at 250 °C, while the S_{BET} of biochar produced at 950 °C was the largest (185.46 m^2/g), which has the potential to be used as adsorbent by means of activation.[33] The pore volumes showed similar trend with that of S_{BET} and reached the maximum at 950 °C. The average pore width of tobacco stem biochar decreased with the increase of temperature. The pore size distribution of tobacco stem biochar (Fig. 3) with the BJH method further confirmed that high temperature biochar mainly consisted of micropores while low temperature biochar mainly included mesopores. The results were in accordance with those of the adsorption and desorption isotherms. As the pyrolysis temperature increased, volatile matter was removed which gave rise to the increase of the surface area and pore volumes. Higher surface area may potentially have a positive influence on agricultural applications of the biochar, and further investigation of this impact on agricultural performance will be tested by adding biochar to soil for practical effects.

TABLE III. Surface area and pore volume of tobacco stem biochar.

Pyrolysis temperature (°C)	BET surface area (m^2/g)	Pore volume of micropore (cm^3/g)	Total pore volume (cm^3/g)	Average pore width (nm)
250	0.1966	0.00080	0.00113	16.2043
350	1.1116	0.00071	0.00370	16.1994
450	1.1725	0.00125	0.00477	16.1734
550	1.0849	0.00187	0.00334	12.3198
650	6.2266	0.00216	0.01221	7.8456
750	24.2762	0.00900	0.02110	3.4762
850	170.1860	0.05533	0.10596	2.4903
950	185.4594	0.06093	0.12077	2.6048

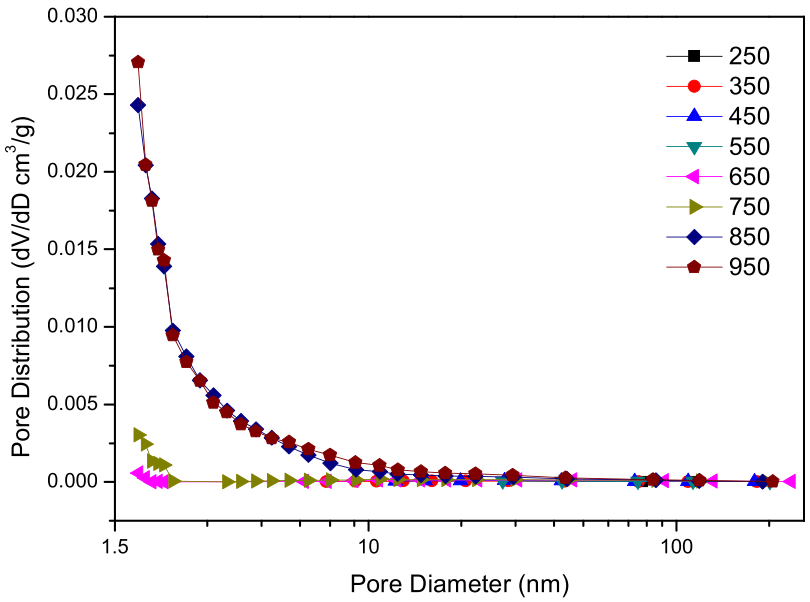

FIG. 3. Pore size distribution of tobacco stem biochar.

2. Evolution of organic functional group

The FTIR spectra for tobacco stem biochar are presented in Fig. 4. The intensity of O-H stretching vibration of the hydroxyl groups decreased with the increase of pyrolysis temperature and almost disappeared after 550 °C. The FTIR spectra at 2930 cm^{-1} were related to C-H stretching vibration, most likely identified as aliphatic CH_3. The peak was relatively weak, reduced with temperature increasing, and was totally disappeared in 450–950 °C biochars. The major FTIR spectra in tobacco stem biochar were observed in the region of 1770–1650 cm^{-1} related to C = O stretching vibration in carbonyl groups, in the region of 1700–1450 cm^{-1} due to C = C stretching vibration representing mostly aromatic compounds, and at the peak of

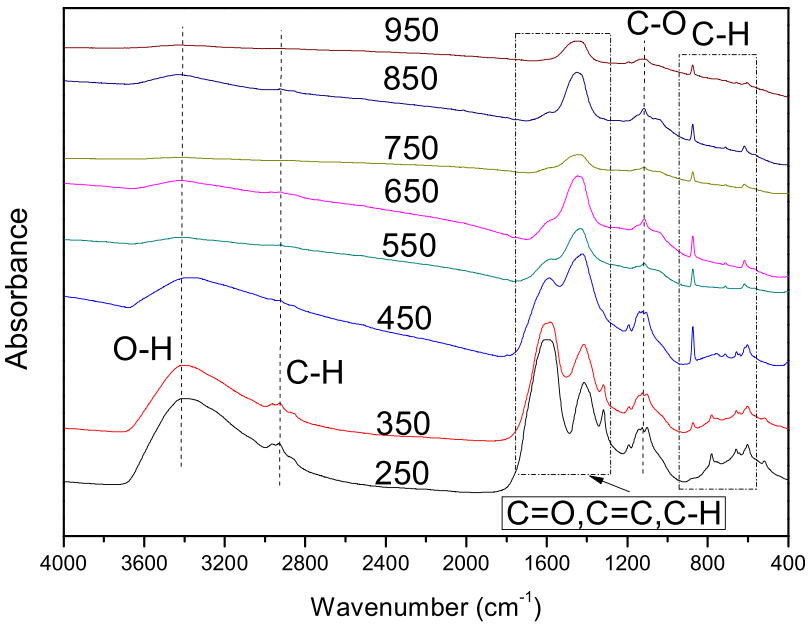

FIG. 4. FTIR spectra of tobacco stem biochar.

1420 cm^{-1} associated with C-H bending vibration. The functional vibrations of C = O and C-H both decreased with pyrolysis temperature, and diminished at 650 °C and 450 °C, respectively. The peak intensity of tobacco stem biochar at 1100 cm^{-1} reduced with pyrolysis temperature, and the groups due to C-O stretching vibration were still presented in biochar produced at 950 °C. It showed that tobacco stem biochar had alcohols, phenols, ethers, and esters groups, and the groups were transformed into a stable bond at higher temperature. The minor peaks observed in the region of 1000 cm^{-1} and 580 cm^{-1} were associated with C-H vibration in alkene and aromatic groups. The different peak positions showed that the structures of functional groups in tobacco stem biochar were different with the increased pyrolysis temperature. Low temperature biochar had much more water sorption functional groups such as carboxy and hydroxy groups, while the major functional groups in high temperature biochar were water repellent.[25,34]

Fig. 5 shows synchronous and asynchronous correlation spectra of tobacco stem biochar pyrolyzed at different temperatures, generated from the temperature-dependent (250, 350, 450,…, 950 °C) spectral variations in the 3700–2800 cm^{-1} and 1800–1000 cm^{-1} regions, respectively. The synchronous spectrum in the 3700–2800 cm^{-1} region developed only one broad auto-peak near 3400 cm^{-1}, which was characteristic of intramolecular hydrogen-bonded OH. The occurrence of the OH stretch vibrations on the $v_1 = v_2$ diagonal of Fig. 5(a) indicated that the bond was subject to change with the increase of pyrolysis temperature. This was consistent with the FTIR spectra of tobacco stem biochar, and the OH groups disappeared at 550 °C. Several asynchronous cross peaks, appearing at the spectral coordinates of 3615, 3440, and 3175 cm^{-1}, indicated that these three IR bands belonged to different hydroxyl groups. Vibration around 3440 cm^{-1} was the same as that at 3400 cm^{-1}, while vibrations around 3615

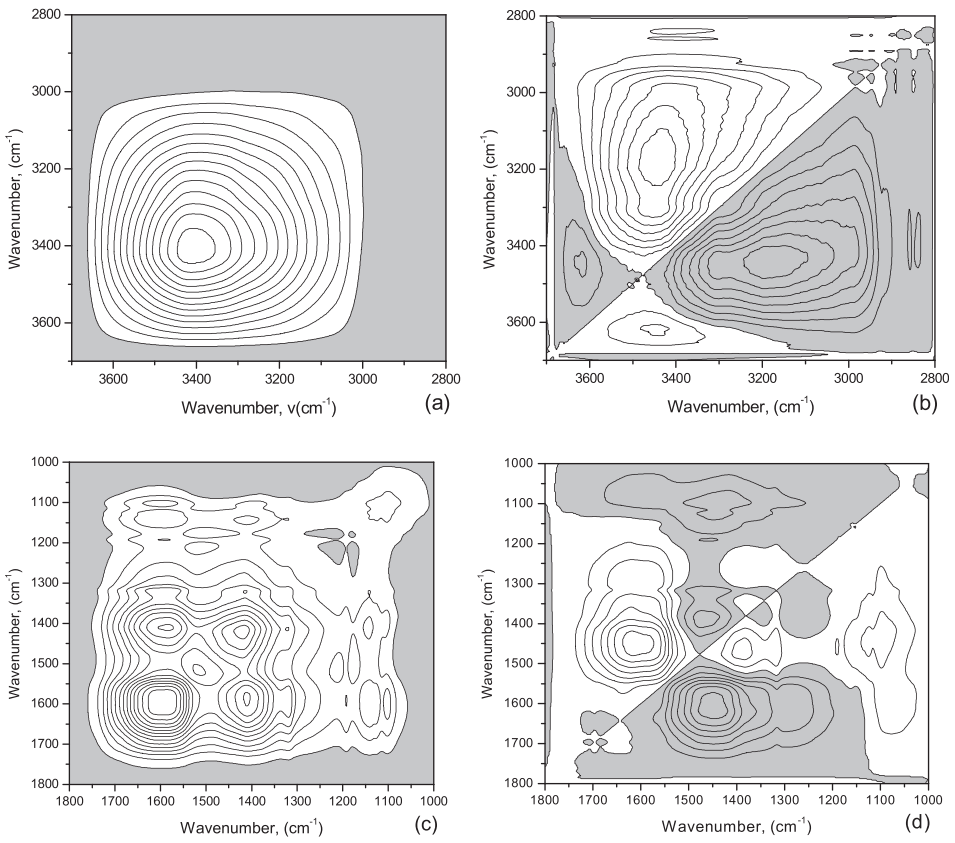

FIG. 5. Synchronous and asynchronous 2D-PCIS spectra in 3700–2800 cm^{-1} (a) and (b) and 1800–1000 cm^{-1} (c) and (d) for tobacco stem biochar between 250 and 950 °C. White and light gray areas indicate positive and negative correlation values, respectively.

and 3175 cm^{-1} were the characteristic of free OH and chelate OH, respectively. The correlation values of Ψ(3440, 3615) and Ψ(3440, 3175) were positive in synchronous correlation spectra, as well as that at the same spectral coordinates in asynchronous correlation spectra. On the basis of Noda's rules,[26] the change of intramolecular hydrogen-bonded OH with the increased temperature diminished earlier than that of free OH and chelate OH. Ψ(2855, 3400) and Ψ(2835, 3400) were observed in the asynchronous correlation spectra which were very weak. The peaks around 2855 and 2835 cm^{-1} were associated with C-H stretching vibration, most likely related to CH_3 on an aromatic ring.[32] The correlation values at (2855, 3400) and (2835, 3400) were both negative in synchronous and asynchronous correlation spectra, suggesting that the demethylation occurred earlier than dehydroxylation with pyrolysis temperature.

The major auto-peaks were observed on the diagonal of the synchronous spectrum (Fig. 5(c)) near 1600, 1514, and 1420 cm^{-1} representing the aromatic skeletal C = C vibrations, O-H bending vibration of aromatic structure, and C-H bending vibration. The absorption intensity of Φ(1600, 1600) was the strongest, followed by Φ(1420, 1420) and Φ(1514, 1514). The cross peak at (1410, 1585) was much stronger in intensity than other cross peaks in the synchronous map, and positive correlation value at Φ(1410, 1585) suggested that the vibrations at 1410 and 1585 cm^{-1} changed simultaneously. Three main cross peaks were observed at (1445, 1600), (1385, 1465), and (1100, 1435) in the asynchronous spectrum. The bands at 1465, 1445, 1435, and 1385 cm^{-1} were reflective of C-H bending vibration, which may belong to different functional groups, and the peak at 1110 cm^{-1} was related to the C-O stretch. The vibration of C = C and C-O stretch occurred earlier than that of C-H bending on the basis of Noda's rules. It further suggested that the functional groups of high temperature biochar possessed strong aromaticity.

3. Inorganic components of tobacco stem biochar

The contents of main inorganic components in biochar are shown in Fig. 6 based on oxides. Biochar obtained from tobacco stem contains a variety of elements for crops such as macroelements (P and K), mid-elements (Ca, Mg, and S), and trace elements (Cl). There are some other metals observed, they are mainly cadmium (1.64%–1.94%), aluminum (0.64%–1.14%), titanium (0.09%–0.17%) oxides with trace elements like copper (0.02%–0.09%), iron (0.15%–0.33%), and

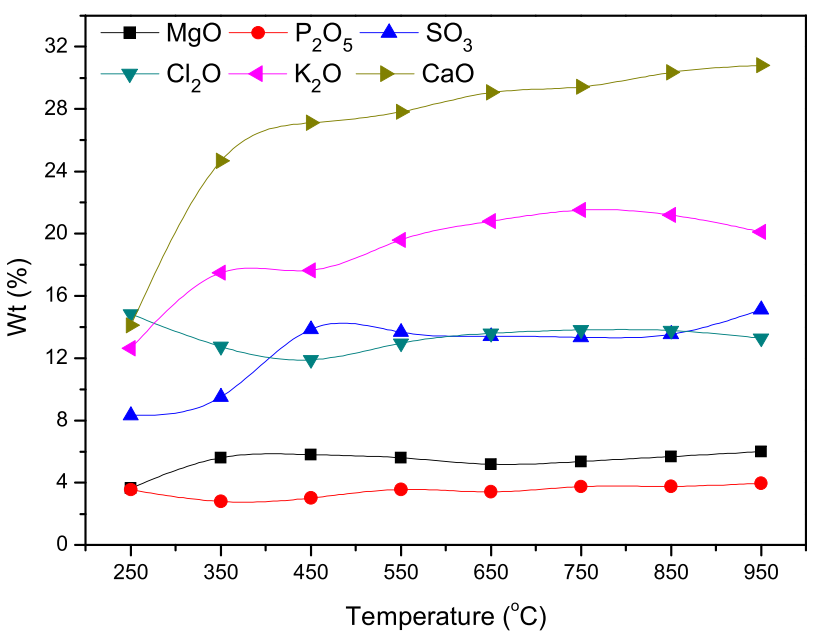

FIG. 6. The contents of inorganic matters in tobacco stem biochar.

manganese (0.13%–0.21%). The contents of these elements were relatively low and changed in a fluctuating way with a small difference after pyrolysis.

The calcium and potassium oxides increased quickly with pyrolysis temperature below 450 °C, and were relatively stable after that. This was likely due to the extensive enrichment of these elements in biochar. The high Ca and K contents in tobacco stem biochar suggest that cultivation of tobacco may have been treated with some fertilizer with calcium and potassium. Apart from Ca and K, the contents of P, Mg, S, and Cl in biochar were higher than those in tobacco stem with the value ranges 2.81%–3.96%, 3.65%–6%, 8.33%–15.12%, and 11.89%–14.84%, respectively. The contents of S and Cl in high temperature biochar were similar which were different from those in low temperature biochar. The S content increased with pyrolysis temperature while Cl decreased at lower temperature. The essential nutrient elements for plant growth measured in biochar indicated that tobacco stem biochar may be a promising material for agricultural applications. However, further research on the availability and speciation of these elements is needed when tobacco stem biochar is considered to be used as soil conditioner and fertilizer carrier.

C. Biochar hygroscopicity

The typical hygroscopicity process of tobacco stem biochar is shown in Fig. 7 with humidity of 70%. It was found that water sorption increased rapidly at first with time extension, and then slowed down gradually until reaching equilibrium. Tobacco stem absorbed the greatest quantity of moisture from the surrounding humid air and the moisture absorption capacity of tobacco stem biochar first decreased and then increased with the increase of pyrolysis temperature, while tobacco stem biochar produced at 550 °C had the lowest hygroscopicity. This may be due to the fact that low temperature biochars had higher O/C and functional groups while high temperature biochars possessed greater surface area. Tobacco stem biochar produced at lower and higher pyrolysis temperatures both had higher hygroscopicity which depended on the physicochemical properties of Tobacco stem biochar.

Tobacco stem and the biochar particles showed higher hygroscopicity. The adsorption curve displayed a steep increase in moisture sorption in the initial stage (Fig. 7, <100 mins), then it reached a gentle moisture increasing by extending the exposure time. However, it

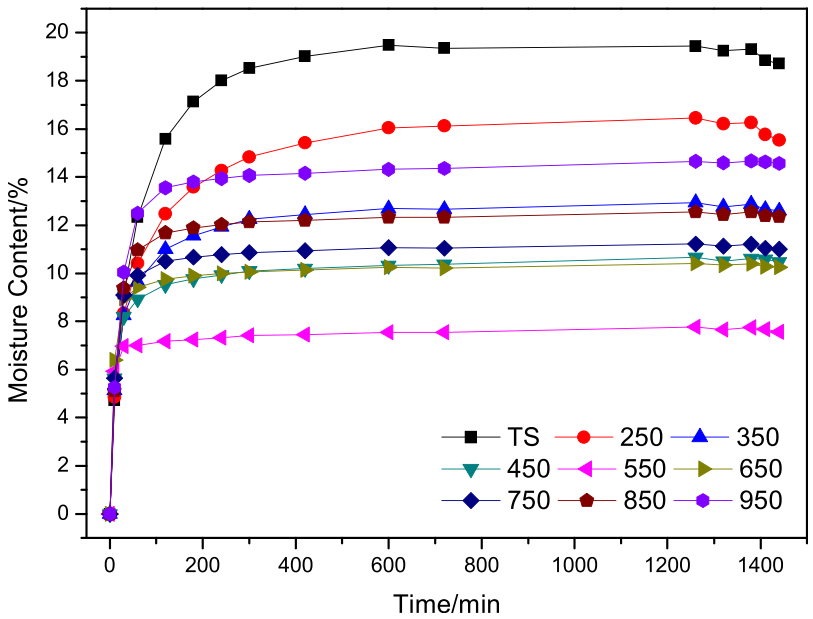

FIG. 7. Moisture adsorption process of tobacco stem biochar at 70% humidity.

took a long time for moisture content of these samples to reach steady state. The moisture sorption rate of tobacco stem biochar at 70% humidity was shown in Fig. 8. The sorption curves of all samples after 10 h almost paralleled to the time axis and the sorption rate approximated to zero, which both signified that the 24 h of moisture sorption process was sufficient for this sorption experiments used in this study. The sorption rates of biochar after 10 min decreased first and then increased with the increased pyrolysis temperature, while there was no evident changing-regular in 10 min. It also showed that the sorption rates reduced quickly in the first 1 h and then it decreased gradually to the zero line. Within the first 2 h, the sorption rate of all samples apart from tobacco stem and its biochar produced at 250 and 350 °C almost reached the stable state. The initial rapid sorption rate indicates that tobacco stem biochars produced at higher experiment will absorb moisture at the fastest rate when they are drier.

Fig. 9 shows EMC of tobacco stem biochar under 50%–70% humidity at 30 °C. The EMC for variant biochar samples showed similar trend with respect to humidity of 50%–70%. It decreased at the beginning and then increased with pyrolysis temperature to the higher range, and it reached the lowest value for biochar derived at 550 °C. It was also found that moisture content was increased with humidity which indicated that the hygroscopicity showed close correlation with the ambient humidity.

The oxygen-containing functional groups and O/C with stronger hygroscopicity decreased first and then disappeared at higher pyrolysis temperature while surface area of biochar increased with the increased pyrolysis temperature. It can be inferred that the hygroscopicity of biochar was affected by the combination of physical adsorption and chemical adsorption. The physical adsorption was one of the main factors affecting the hygroscopicity of biochar at lower humidity, and the influence of chemical adsorption increased with the increasing of the humidity. High temperature biochar with greater surface area had strong physical adsorption while the water-absorbing capacity of low temperature biochar was mainly controlled by chemical adsorption. It can be considered that biochar produced at 550 °C has the lowest hygroscopicity under 50%–70% humidity which may be used as a hydrophobic material while tobacco stem biochar produced at the temperature lower than 450 °C with higher hygroscopicity may help the soil hold moisture and nutrients, and biochar produced at temperature higher than 650 °C can be designed as the raw material for activated carbon.

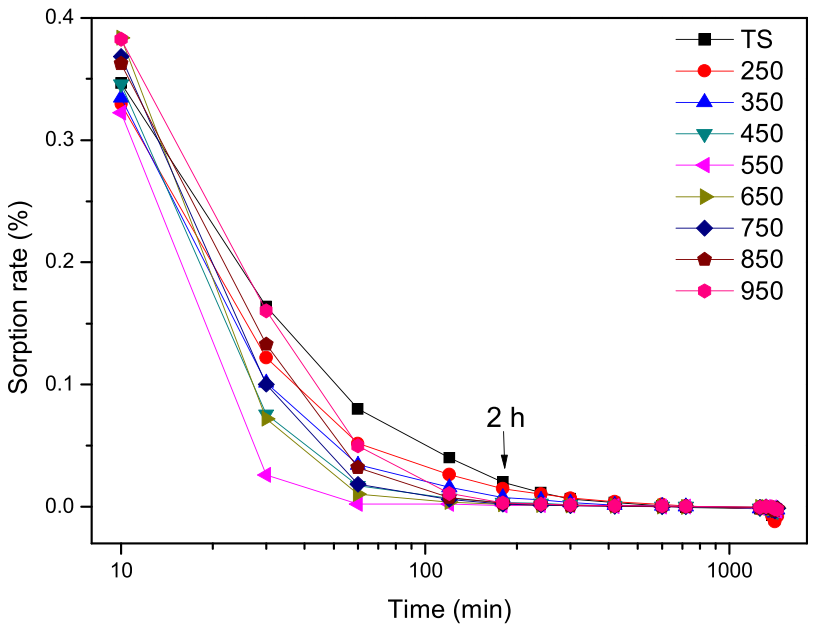

FIG. 8. Moisture sorption rate of tobacco stem biochar at the humidity of 70%.

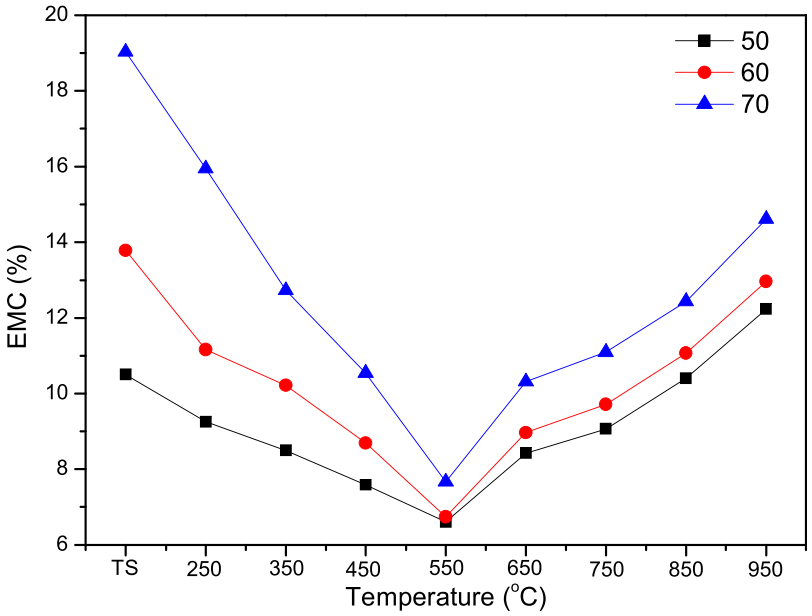

FIG. 9. EMC of tobacco stem biochar with various humidity at 30 °C.

IV. CONCLUSION

The results of this study showed that the yields and physicochemical properties of biochars from tobacco stem pyrolysis were greatly dependent on pyrolysis temperature. The yield of tobacco stem biochar decreased continuously from 52.39% at 250 °C to 23.29% at 950 °C. Tobacco stem biochar is not suitable to be used as fuel due to its low LHV, low fixed carbon, high volatile matter, and high ash content. It had high hygroscopicity at higher humidity, and water absorbing capacity was first decreased and then increased with the increasing pyrolysis temperature. Future studies should focus on the high value-added utilization of tobacco stem biochar for a specific purpose.

ACKNOWLEDGMENTS

The authors greatly appreciate the financial support from the National Natural Science Foundation of China (51376075, 51376076), the Special Fund for Agro-scientific Research in the Public Interest (201303095), and the Foundation of State Key Laboratory of Coal Combustion (FSKLCCB1504). The experiment was also assisted by Analytical and Testing Center in Huazhong University of Science and Technology (http://atc.hust.edu.cn).

[1]J. Lehmann, M. C. Rillig, J. Thies, C. A. Masiello, W. C. Hockaday, and D. Crowley, Soil Biol. Biochem. **43**, 1812 (2011).
[2]F. G. A. Verheijen, S. Jeffery, A. C. Bastos, M. van der Velde, and I. Diafas, Biochar Application to Soils - A Critical Scientific Review of Effects on Soil Properties, Processes and Functions. EUR 24099 EN, Office for the Official Publications of the European Communities, Luxembourg, p. 149 (2009).
[3]J. Major, M. Rondon, D. Molina, S. J. Riha, and J. Lehmann, Plant Soil **333**, 117 (2010).
[4]S. S. Akhtar, G. Li, M. N. Andersen, and F. Liu, Agric. Water Manage. **138**, 37 (2014).
[5]J. Lehmann, J. Gaunt, and M. Rondon, *Mitigation and Adaptation Strategies for Global Change* (Springer, 2006), Vol. 11, p. 395.
[6]S. Sohi, E. Lopez-Capel, E. Krull, and R. Bol, CSIRO Land and Water Science Report No. 5 (2009), p. 17.
[7]D. Kolodynska, R. Wnetrzak, J. J. Leahy, M. H. B. Hayes, W. Kwapinski, and Z. Hubicki, Chem. Eng. J. **197**, 295 (2012).
[8]D. Mohan, A. Sarswat, Y. S. Ok, and C. U. Pittman, Jr., Bioresour. Technol. **160**, 191 (2014).
[9]J. Gaskin, C. Steiner, K. Harris, K. Das, and B. Bibens, Trans. ASABE **51**, 2061 (2008).
[10]S. Kloss, F. Zehetner, A. Dellantonio, R. Hamid, F. Ottner, V. Liedtke, M. Schwanninger, M. H. Gerzabek, and G. Soja, J. Environ. Qual. **41**, 990 (2012).
[11]Y. Sun, B. Gao, Y. Yao, J. Fang, M. Zhang, Y. Zhou, H. Chen, and L. Yang, Chem. Eng. J. **240**, 574 (2014).
[12]A. Demirbas and G. Arin, Energy Source **24**, 471 (2002).

[13]D. Vamvuka, Int. J. Energy Res. **35**, 835 (2011).
[14]H. Zheng, Z. Wang, X. Deng, J. Zhao, Y. Luo, J. Novak, S. Herbert, and B. Xing, Bioresour. Technol. **130**, 463 (2013).
[15]M. I. Al-Wabel, A. Al-Omran, A. H. El-Naggar, M. Nadeem, and A. R. A. Usman, Bioresour. Technol. **131**, 374 (2013).
[16]J. M. Novak, I. Lima, B. Xing, J. W. Gaskin, C. Steiner, K. Das, M. Ahmedna, D. Rehrah, D. W. Watts, and W. J. Busscher, Ann. Environ. Sci. **3**, 195 (2009).
[17]C. R. Cardoso, M. R. Miranda, K. G. Santos, and C. H. Ataide, J. Anal. Appl. Pyrolysis **92**, 392 (2011).
[18]E. Apaydin-Varol and A. E. Putun, J. Anal. Appl. Pyrolysis **98**, 29 (2012).
[19]W. Gao, K. Chen, Z. Xiang, F. Yang, J. Zeng, J. Li, R. Yang, G. Rao, and H. Tao, Ind. Crops Prod. **44**, 152 (2013).
[20]O. Senneca, S. Ciaravolo, and A. Nunziata, J. Anal. Appl. Pyrolysis **79**, 234 (2007).
[21]B. Liu, Y.-M. Li, S.-B. Wu, Y.-H. Li, S.-S. Deng, and Z.-L. Xia, BioResources **8**, 220 (2012).
[22]V. Strezov, E. Popovic, R. V. Filkoski, P. Shah, and T. Evans, Energy Fuels **26**, 5930 (2012).
[23]K. Karhu, T. Mattila, I. Bergstrom, and K. Regina, Agric. Ecosyst. Environ. **140**, 309 (2011).
[24]R. S. Vartapetyan and A. Voloshchuk, Russ. Chem. Rev. **64**, 985 (1995).
[25]T. J. Kinney, C. A. Masiello, B. Dugan, W. C. Hockaday, M. R. Dean, K. Zygourakis, and R. T. Barnes, Biomass Bioenergy **41**, 34 (2012).
[26]I. Noda, A. Dowrey, C. Marcott, G. Story, and Y. Ozaki, Appl. Spectrosc. **54**, 236 (2000).
[27]O. R. Harvey, B. E. Herbert, L. J. Kuo, and P. Louchouarn, Environ. Sci. Technol. **46**, 10641 (2012).
[28]H. Yang, B. Liu, Y. Chen, B. Li, and H. Chen, Energy Fuels **29**, 7327 (2015).
[29]Y. Chen, H. Yang, X. Wang, S. Zhang, and H. Chen, Bioresour. Technol. **107**, 411 (2012).
[30]D. Ozcimen and A. Ersoy-Mericboyu, Renewable Energy **35**, 1319 (2010).
[31]K. S. W. Sing, Pure App. Chem. **57**, 603 (1985).
[32]R. K. Sharma, J. B. Wooten, V. L. Baliga, P. A. Martoglio-Smith, and M. R. Hajaligol, J. Agric. Food Chem. **50**, 771 (2002).
[33]X. Zhang, S. Zhang, H. Yang, J. Shao, Y. Chen, Y. Feng, X. Wang, and H. Chen, Energy **91**, 903 (2015).
[34]Y. Chun, G. Sheng, C. T. Chiou, and B. Xing, Environ. Sci. Technol. **38**, 4649 (2004).